OPEN

Citation: Cell Death and Disease (2014) 5, e1056; doi:10.1038/cddis.2014.33

www.nature.com/cddis

Nonthermal plasma induces head and neck cancer cell death: the potential involvement of mitogen-activated protein kinase-dependent mitochondrial reactive oxygen species

SU Kang[1], J-H Cho[2], JW Chang[1], YS Shin[1], KI Kim[3], JK Park[1], SS Yang[3], J-S Lee[4], E Moon[4], K Lee[5] and C-H Kim*[,1]

Nonthermal plasma (NTP) is generated by ionization of neutral gas molecules, which results in a mixture of energy particles including electrons and ions. Recent progress in the understanding of NTP has led to its application in the treatment of various diseases, including cancer. However, the molecular mechanisms of NTP-induced cell death are unclear. The purpose of this study was to evaluate the molecular mechanism of NTP in the induction of apoptosis of head and neck cancer (HNC) cells. The effects of NTP on apoptosis were investigated using MTT, terminal deoxynucleotidyl transferase-mediated dUTP-biotin nick-end labeling, Annexin V assays, and western blot analysis. The cells were examined for production of reactive oxygen species (ROS) using DCFCA or MitoSOX staining, intracellular signaling, and an animal model. NTP reduced HNC cell viability in a dose-dependent manner and induced apoptosis. NTP resulted in alteration of mitochondrial membrane potential and accumulation of intracellular ROS generated from the mitochondria in HNC cells. Blockade of ROS production by *N*-acetyl-L-cysteine inhibited NTP-induced apoptosis. NTP led to the phosphorylation of c-JUN N-terminal kinase (JNK) and p38, but not extracellular-regulated kinase. Treatment with JNK and p38 inhibitors alleviated NTP-induced apoptosis via ROS generation. Taken together, these results show that NTP induced apoptosis of HNC cells by a mechanism involving MAPK-dependent mitochondrial ROS. NTP inhibited the growth of pre-established FaDu tumors in a nude mouse xenograft model and resulted in accumulation of intracellular ROS. In conclusion, NTP induced apoptosis in HNC cells through a novel mechanism involving MAPK-mediated mitochondrial ROS. These findings show the therapeutic potential of NTP in HNC.
Cell Death and Disease (2014) **5,** e1056; doi:10.1038/cddis.2014.33; published online 13 February 2014
Subject Category: Cancer

Head and neck cancer (HNC) is the fifth most common cancer worldwide.[1] Despite technical advances in surgery, radiotherapy, and chemotherapy, survival rates have remained virtually unchanged over the past 50 years in patients with advanced HNC.[2] Therefore, a new modality for treatment of HNC is needed to improve survival and decrease toxicity.

Nonthermal plasma (NTP) is being investigated in terms of its biomedical application and has recently emerged as a novel tool in cancer treatment. The anticancer activity of NTP has been demonstrated in several *in vitro* and *in vivo* animal models, including skin, liver, and colon cancers.[3–5] Plasma is an ionized gas composed of charged particles, electronically excited atoms and molecules, radicals, and UV photons. The effects of NTP are owing to the active species, mainly oxygen/hydroxyl radicals and nitric oxide, that are generated in the plasma or tissue brought into contact with NTP.[6,7]

Acting as primary coordinators of the apoptotic processes, reactive oxygen species (ROS) generated by NTP can mediate apoptosis of mammalian cancer cells by mitochondrial dysfunction.[7,8] Free radicals have important roles in a number of biological processes and have also been implicated in cellular redox signaling. However, excessive amounts of free radicals secondary to an imbalance of the redox milieu can lead to cell damage and death.[9] It has been increasingly reported that DNA damage and reactive species generated by NTP could be the main causes of apoptosis in various types of cancer.[4,5,10,11]

However, the molecular mechanism of the particular NTP that induces apoptosis and the specific signals that stimulate NTP-induced apoptosis remain unclear. In this study, we investigated whether NTP in HNC cells causes ROS-induced apoptosis, along with the molecular signals involved.

Results

Analysis of NTP on cell death and apoptotic effect. A gas (helium and oxygen)-only treatment was used as a control to

[1]Department of Otolaryngology, Ajou University School of Medicine, Suwon, Gyounggi-Do, Korea; [2]Department of Otorhinolaryngology-Head Neck Surgery, The Catholic University, Suwon, Gyounggi-Do, Korea; [3]Department of Electrical and Computer Engineering, Ajou University, Suwon, Gyounggi-Do, Korea; [4]Department of Molecular Science and Technology and Department of Life Science, Ajou University, Suwon, Gyounggi-Do, Korea and [5]PSM America Inc., Colorado Springs, CO, USA
*Corresponding author: C-H Kim, Department of Otolaryngology, Ajou University School of Medicine, 5 Wonchon-Dong, Yeongtong-Gu, Suwon 442-749, Gyounggi-Do, Korea. Tel: +82 31 219 5269; Fax: +82 31 219 5264; E-mail: ostium@ajou.ac.kr
Keywords: nonthermal plasma; apoptosis; MAPK; ROS; head and neck cancer
Abbreviations: ERK, extracellular-regulated kinase; FACS, fluorescence-activated cell sorting; HNC, head and neck cancer; JNK, c-JUN N-terminal kinase; MAPK, mitogen-activated protein kinase; MEM, minimum essential medium; MMP, mitochondrial membrane potential; NAC, *N*-acetyl cysteine; NTP, nonthermal plasma; ROS, reactive oxygen species; SCC, squamous cell carcinoma; TUNEL, terminal deoxynucleotidyl transferase-mediated dUTP-biotin nick-end labeling
Received 09.11.13; revised 06.1.14; accepted 16.1.14; Edited by A Finazzi-Agró

exclude the gas effects of NTP. Gas-only treatment did not show any significant effect on cell viability. NTP treatment of FaDu cells (2 kV for 1 s (15.7%) and 4 kV for 1 s (29.1%)) resulted in a significant increase in apoptosis compared with the control (5.1%) and gas-only (7.8%) groups (Figure 1b). Consistent with the Annexin V assay results of FaDu cells, treatment with NTP resulted in increased apoptosis of HN9, SNU899, and SNU1041 cells (Figure 1b). In addition, NTP treatment significantly increased the number of terminal deoxynucleotidyl transferase-mediated dUTP-biotin nick-end labeling (TUNEL)-positive cells, indicating that NTP indeed induces apoptosis in FaDu cells (Figure 1c).

Activation of the mitogen-activated protein kinase pathway in FaDu cells treated with NTP. Next, we investigated the activation of apoptotic signal molecules in NTP-treated cells. Increased expression of p-p38, p-c-JUN N-terminal kinase (JNK), and p-extracellular-regulated kinase (ERK) was detected after NTP treatment in FaDu cells. Moreover, the dose-dependent activation of PARP and cleaved caspase-3 was associated with NTP-induced apoptosis of FaDu cells (Figure 1d).

Increased ROS generation and loss of mitochondrial dysfunction are involved in NTP-induced apoptosis. An approximate twofold increase in intracellular peroxide levels was found in cells treated with NTP compared with the controls (Figure 2a). Next, to determine whether the ROS induced by NTP was generated in the mitochondria, we stained plasma-treated cells with MitoSOX and performed fluorescence-activated cell sorting (FACS) analysis. Mitochondrial superoxide levels were increased in NTP-treated cells. In addition, confocal microscopy images showed that the MitoSOX (stained red) colocalized with the mitochondria-staining

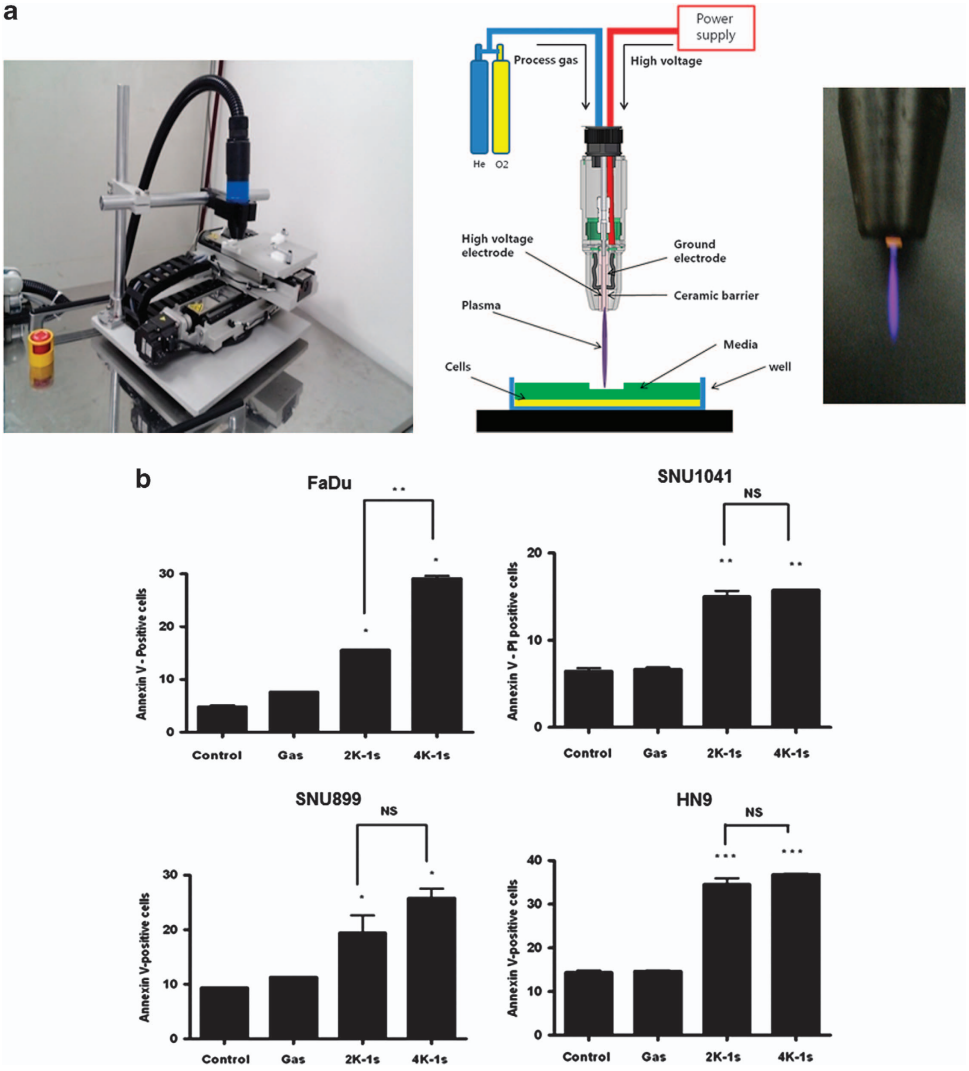

Figure 1 Apoptotic effects of NTP on HNC cells. (**a**) Photograph of a plasma jet, schematic diagram of the plasma system, and image of a plasma jet. (**b**) Various HNC cells were analyzed 24 h after treatment with NTP by staining with Annexin V/PI. (**c**) Apoptosis of FaDu cells was determined by the TUNEL method using a detection kit. (**d**) The cell lysates were then separated by SDS-PAGE and immunoblotted with anti-p-JNK, p-p38, p-ERK, cleaved caspase-3, and PARP antibodies. Scale bar denotes 50 μm. $^{*}P<0.05$, $^{**}P<0.01$, and $^{***}P<0.001$

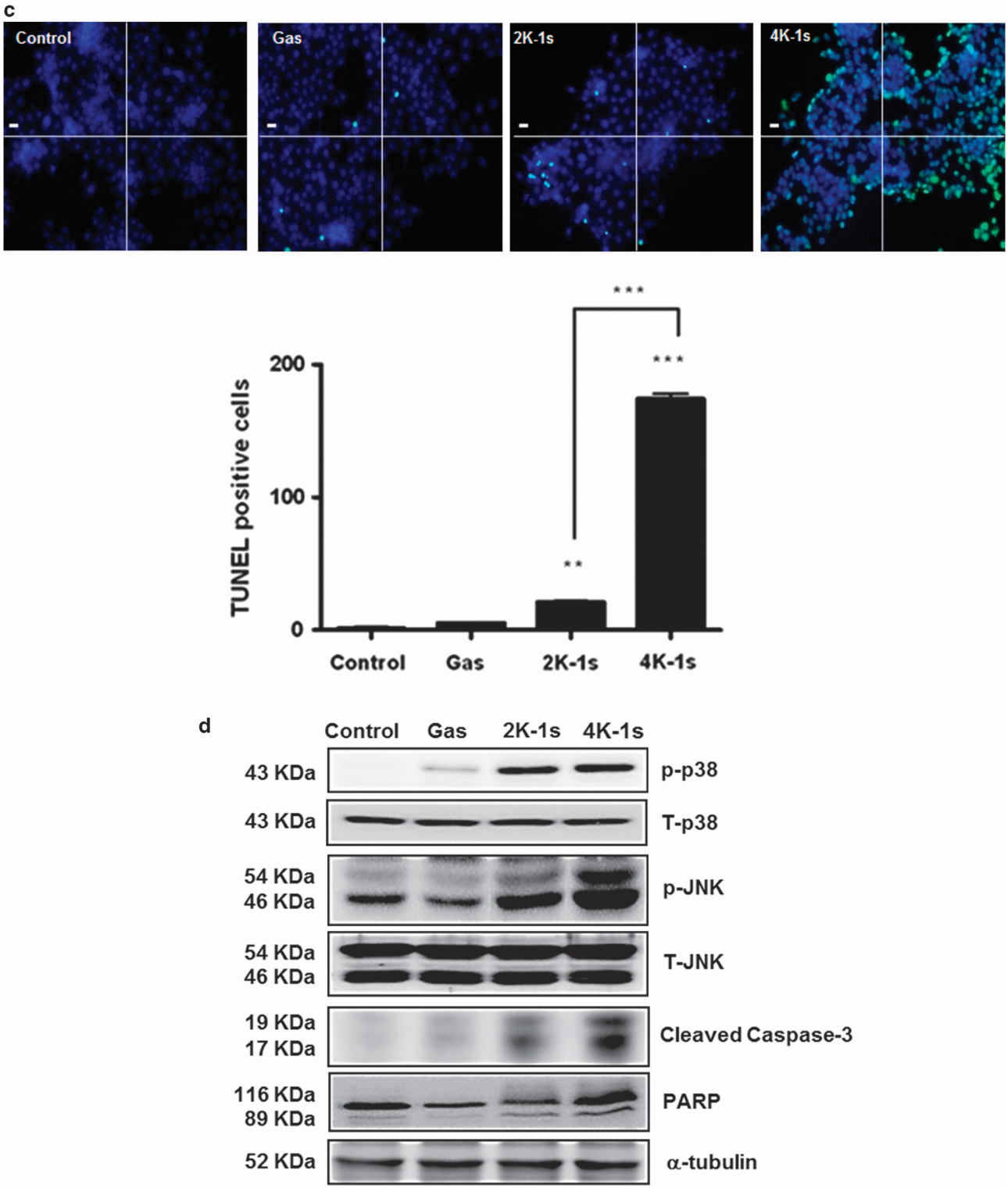

Figure 1 (Continued)

dye MitoTracker (green) (merged as yellow in Figure 2b), confirming that the ROS were generated by the mitochondria.

In the mitochondrial membrane potential (MMP) measurement, NTP increased the green fluorescence of cells, indicating a loss of MMP and mitochondrial damage (Figure 2c). Taken together, these results show that NTP induced apoptosis via mitochondrial ROS generation and mitochondrial dysfunction.

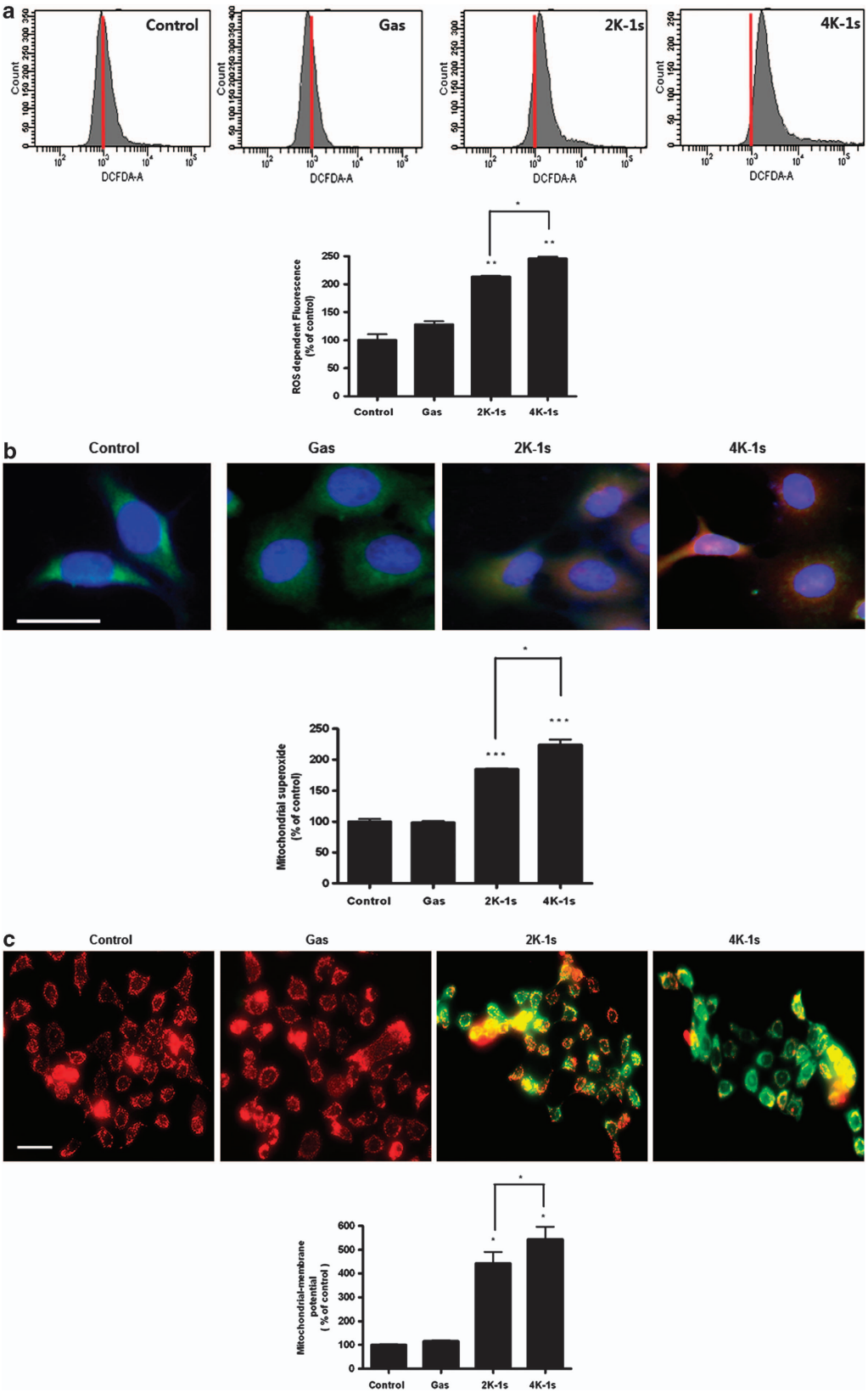

Figure 2 Induction of ROS in NTP-treated FaDu cells. (**a**) FaDu cells were treated with DCFDA and assayed using flow cytometry. (**b**) For measurement of mitochondrial superoxide, the cells were incubated with 2.5 μM of MitoSOX and then stained with 180 nM MitoTracker. (**c**) MMP was measured by flow cytometry using JC-1 fluorescence. Scale bar denotes 50 μm. $^{*}P<0.05$, $^{**}P<0.01$, and $^{***}P<0.001$

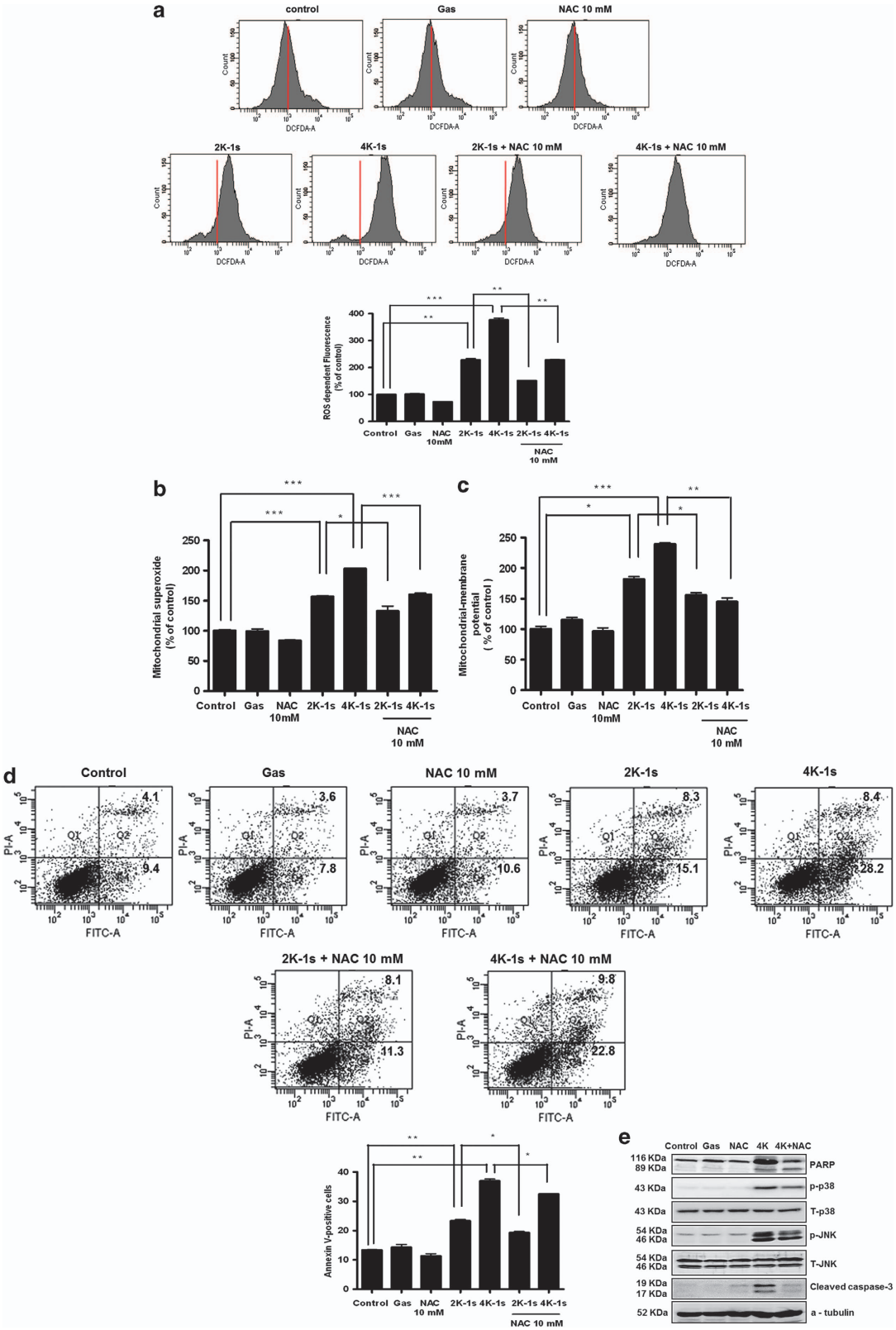

Figure 3 Effect of NTP-generated ROS on apoptosis. Cells were treated with NAC (10 mM) for 1 h before treatment with NTP. (**a**) Measurement of ROS generation using flow cytometry. (**b**) Measurement of mitochondrial superoxide with MitoSOX and MitoTracker. (**c**) Measurement of MMP with JC-1. (**d**) Analysis of apoptosis by FACS with Annexin V-PI. (**e**) The cell lysates were assessed by western blot analysis using antibodies against p-JNK, p-p38, p-ERK, cleaved caspase-3, and PARP. $^{*}P<0.05$, $^{**}P<0.01$, and $^{***}P<0.001$

Antioxidants alleviate apoptosis following NTP treatment. We determined whether the ROS generated by NTP are implicated in NTP-mediated apoptosis. *N*-acetyl cysteine (NAC) is a well-known thiol antioxidant. In combination with NTP and NAC, the levels of ROS generation, mitochondria superoxide, and MMP were significantly lower than those of NTP-treated cells (Figures 3a–c). In combination with NAC treatment, apoptosis induced by NTP was alleviated compared with the control and gas groups (Figure 3d). In a similar manner, NAC attenuated the apoptotic effect of NTP (Figure 3d). These findings suggest that removal of ROS can abrogate NTP-induced cell death and that ROS mediate NTP-induced apoptosis.

To examine the relationship between the role of ROS and the underlying mechanism of apoptosis induced by NTP, we determined whether the NTP-induced apoptotic pathway was

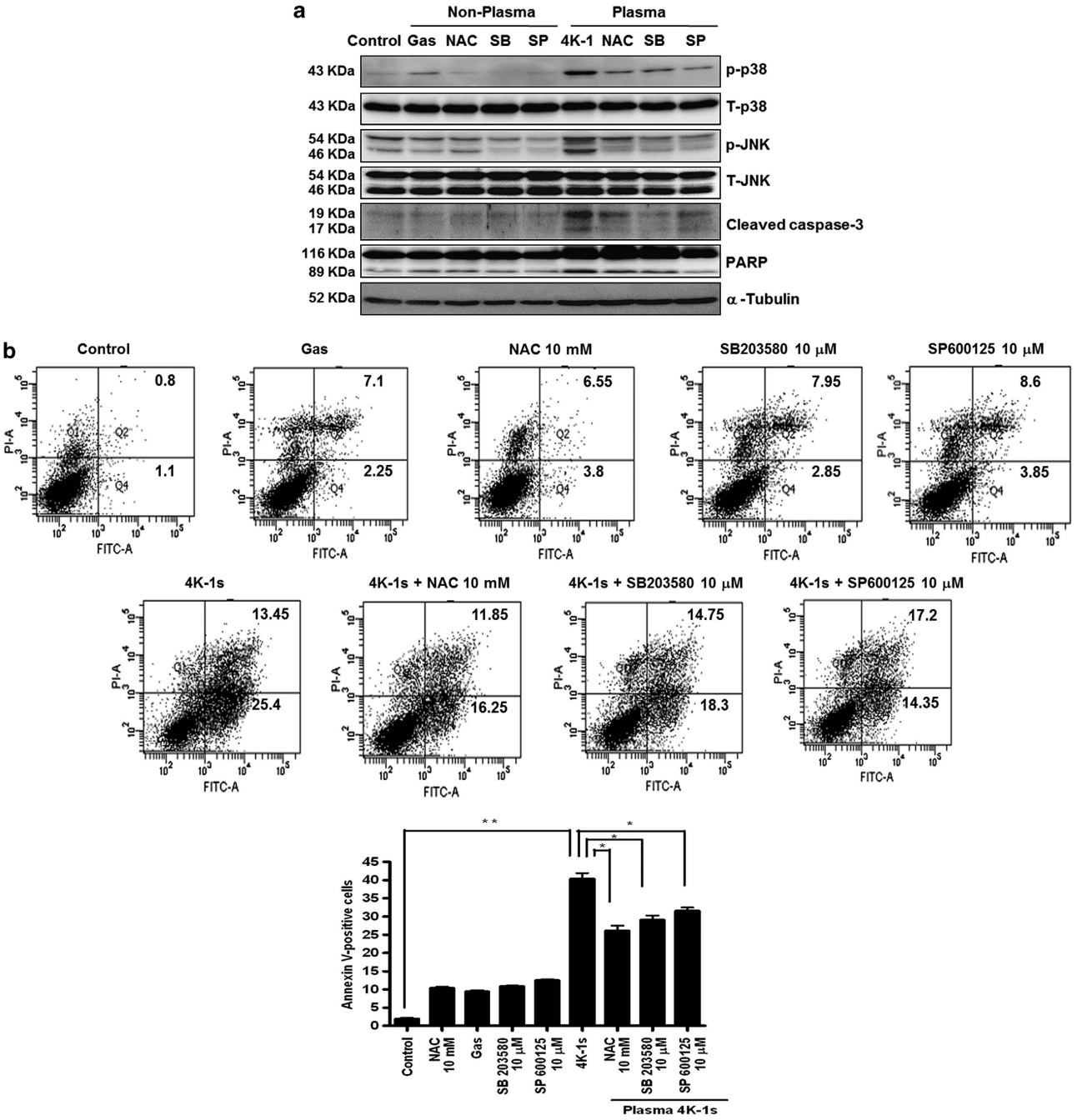

Figure 4 Involvement of MAPK in the generation of mitochondrial ROS and mitochondrial dysfunction. Apoptosis of FaDu cells was assessed 24 h after NTP with or without preincubation with NAC (10 mM), SB2023580 (10 μM), or SP 600125 (10 μM). (**a**) Immunoblotting was performed using antibodies against p-JNK, p-p38, p-ERK, cleaved caspase-3, and PARP. (**b**) Analysis of apoptosis by FACS with Annexin V-PI. (**c**) Measurement of ROS generation by flow cytometry. (**d**) Measurement of mitochondrial superoxide using MitoSOX and MitoTracker. (**e**) Measurement of MMP using JC-1. *$P<0.05$, **$P<0.01$, and ***$P<0.001$

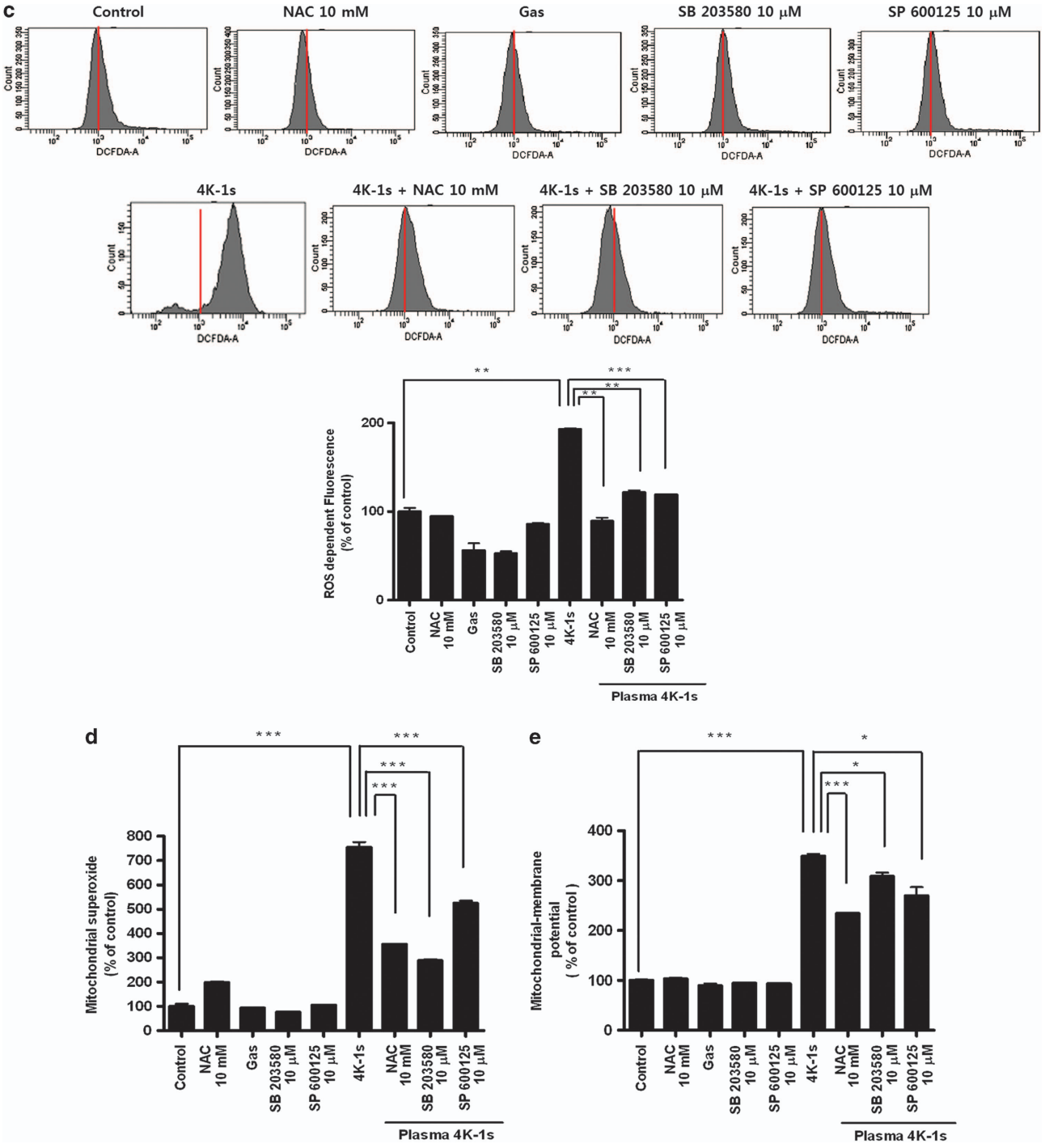

Figure 4 (Continued)

inhibited by NAC. Interestingly enough, as shown in Figure 3e, the increased expression of cleaved caspase-3 and PARP by NTP was attenuated by NAC pretreatment. Furthermore, NAC prevented NTP-mediated p-p38 and p-JNK expression.

Mitogen-activated protein kinase involves generation of mitochondrial ROS and mitochondrial dysfunction in NTP-induced apoptosis. We used NAC and specific inhibitors for JNK (SP600125) and p-38 (SB203580) to further confirm the involvement of ROS and the mitogen-activated protein kinase (MAPK) signaling pathway in NTP-induced apoptosis. Activated caspase-3 and the specific cleavage of PARP were identified in cells treated with NTP for 24 h, followed by the activation of JNK and p38. Cotreatment with NAC, SP600125, or SB203580 reduced the expression of p-JNK and p-p38, leading to decreased cleavage of caspase-3 and PARP (Figure 4a). As shown in Figure 4b, when cells were treated with NAC, SP600125, or

SB203580 in combination with NTP, the percentage of apoptosis was reduced significantly when compared with combined treatment. Approximately 39% of cells were undergoing apoptotic death after NTP treatment; however, cotreatment with NAC, SP600125, or SB203580 reduced this to 28.1%, 23.05%, and 31.55%, respectively (Figure 4b). Furthermore, levels of ROS generation, mitochondria superoxide, and MMP were significantly lower than those in the NTP-treated cells (Figures 4c–e).

These findings suggest that removal of ROS can abrogate NTP-induced cell death and that ROS mediate the NTP-induced apoptosis. These results also suggest that NTP induces apoptosis via downregulation of p38 and JNK.

NTP treatment inhibits tumor growth and induces apoptosis *in vivo*. NTP significantly suppressed the tumor growth after 11 days of treatment (Figure 5a). In addition, the volume and weight of the tumors were decreased by NTP (Figures 5b and c). Figure 5d reveals that tumor tissue from the NTP-treated mice showed increased caspase-3 and Nox-3 levels, and TUNEL staining, compared with control tissue. Therefore, these results suggest that NTP more effectively inhibited tumor growth than did the control, and that ROS mediated the NTP-induced apoptosis *in vivo*, as observed *in vitro*.

Discussion

Several recent studies revealed that NTP can induce cancer cell apoptosis in a dose-dependent manner and that this might be related to DNA damage resulting from the generation of ROS.[11,12] Also, they present preferential killing of cancer cells over the normal cells by NTP.[11,12]

HNCs usually begin in the squamous cells that line the mucosal surface of head and neck area. Therefore, HNC can be approached and managed via natural orifice (oral and nasal cavity). Thus, we hypothesized that if NTP can induce cell death in the HNC cells, it could be a novel way to treat locoregional head and neck squamous cell carcinoma (SCC) or premalignant lesion. NTP can be a promising adjuvant modality to handle microinvolvement of tumor after surgical resection.

ROS seem to be indispensable for the signal-transduction pathways that regulate cell growth and the redox status. However, overproduction of ROS can damage lipids, proteins, and DNA. This study demonstrated that intracellular ROS production was increased significantly by NTP treatment. An increase in ROS and a consequent loss of MMP were reported to be typical phenomena during mitochondria-dependent apoptosis.[13] Loss of MMP also induces apoptosis by causing the release of proapoptotic factors, such as cytochrome *c*, from the mitochondrial inner space to the cytosol.[14] Cytochrome *c* release from the mitochondria can activate caspase-9, which in turn activates executioner caspase-3 via cleavage induction.[15] This idea is strongly supported by the fact that the antioxidant NAC effectively blocked the NTP-induced activation of apoptosis-related proteins and the decline in cellular viability.

MAPKs are mediators of cellular responses to extracellular signals, including ERK 1/2, JNK, and p38. The results of our study showed that NTP caused activation of JNK and p38 rather than ERK. Generally, activation of ERK enhances cell proliferation, while activation of JNK and p38 facilitates cell death.[16] In the present study, we performed an inhibitor study of p38 and JNK to elucidate the roles of MAPK involved in NTP-induced apoptosis. The JNK inhibitor (SP600125) and the p38 inhibitor (SB203580) reversed the NTP-induced activation of caspase-3. The inhibitor assay showed that blockade of JNK and p38 activation largely rescued plasma-induced apoptosis and significantly decreased the levels of ROS generation, mitochondria superoxide, and MMP. In addition, these results indicate that the phosphorylation of JNK and p38 can be suppressed by NAC.

This is the first study to evaluate the molecular signals involved in ROS-induced apoptosis by NTP in HNC. In conclusion, our data show that NTP induces dose-dependent cell apoptosis via ROS production. It may induce apoptosis of HNC cells through a ROS/MAPK-mediated mitochondrial pathway. These findings provide insight into the mechanism underlying NTP-mediated apoptosis.

Materials and Methods

Cell lines and reagents. FaDu and SNU1041, SCC lines that originated from human hypopharynx, SNU899, originating from human laryngeal SCC, and HN9, established from an undifferentiated carcinoma of the parotid gland, were used. FaDu was purchased from the American Type Culture Collection (ATCC, Manassas, VA, USA), and SNU1041 and SNU899 cells were from the Korean Cell Line Bank (KCLB, Seoul, Korea). HN9 was kindly provided by Dr. Sang-Yoon Kim (Asan Medical Center, University of Ulsan College of Medicine, Ulsan, Korea). FaDu and HN9 cells were grown in minimum essential medium (MEM; Gibco, Carlsbad, CA, USA), whereas SNU899 and SNU1041 were maintained in RPMI 1640 medium (Gibco), supplemented with 10% fetal bovine serum and 100 U/ml penicillin–streptomycin (Gibco). The cells were maintained at 37 °C with 5% CO_2 under humidified conditions.[17] NAC was purchased from Sigma Chemical Inc. (St. Louis, MO, USA). SB203580 and SP600125 were purchased from Calbiochem (San Diego, CA, USA).

Experimental system specifications and NTP treatment. We designed and manufactured a spray-type atmospheric pressure NTP system with a newly designed arc-free and antistatic plate to provide uniform NTP for biological research applications (Figure 1a).[5] The plasma source is equipped with a pair of electrodes that is made of Al_2O_3 (high voltage and ground electrodes, $10 \times 40\,mm^2$ dimension, 2 mm gap between electrodes) that is isolated from direct contact with the plasma by a ceramic barrier. The specifications of the power supply with this system are 2 kV minimum, 13 kV maximum, and mean frequency 20–30 kHz; these specifications can vary with the type and amount of gas used. In this study, helium and oxygen were used as carrier gases because we previously found that the addition of O_2 to an He plasma improved the efficiency of cancer cell inhibition.[3,5] The voltage and current of NTP were measured uniformly and stably. The plasma density, in our study, using $He + O_2$ as a carrier gas was calculated as $\sim 10^6/m^3$ by optical emission spectroscopy, and the ROS density was $\sim 10^{13}/m^3$. The temperature of plasma gas was kept low at ~ 35 °C even after 10 min treatment at 13 kV for NTP treatment.

For NTP treatment, we used 3 ml of cell suspension with a concentration of 1×10^5 cells/ml on the petridish (diameter ~ 60 mm, 10060; SPL, Pochen-Si, Gyeonggi-do, Korea). The depth of media was about 10 mm, and we kept the distance between the plasma device and the bottom of petridish ~ 3 cm. The NTP jet partially dispel a media, but not all.

Annexin V and propidium iodide staining. Cell death was detected using an FITC Annexin V-PE apoptosis detection kit I according to the manufacturer's protocol (BD Biosciences, Bedford, MA, USA), as described previously.[18] Briefly, cells were treated with gas-only or plasma jets for 2 or 4 V for 1 s and then incubated further for 24 h. The cells were harvested, washed with PBS, and stained with Annexin V-FITC and propidium iodide (PI). The early and

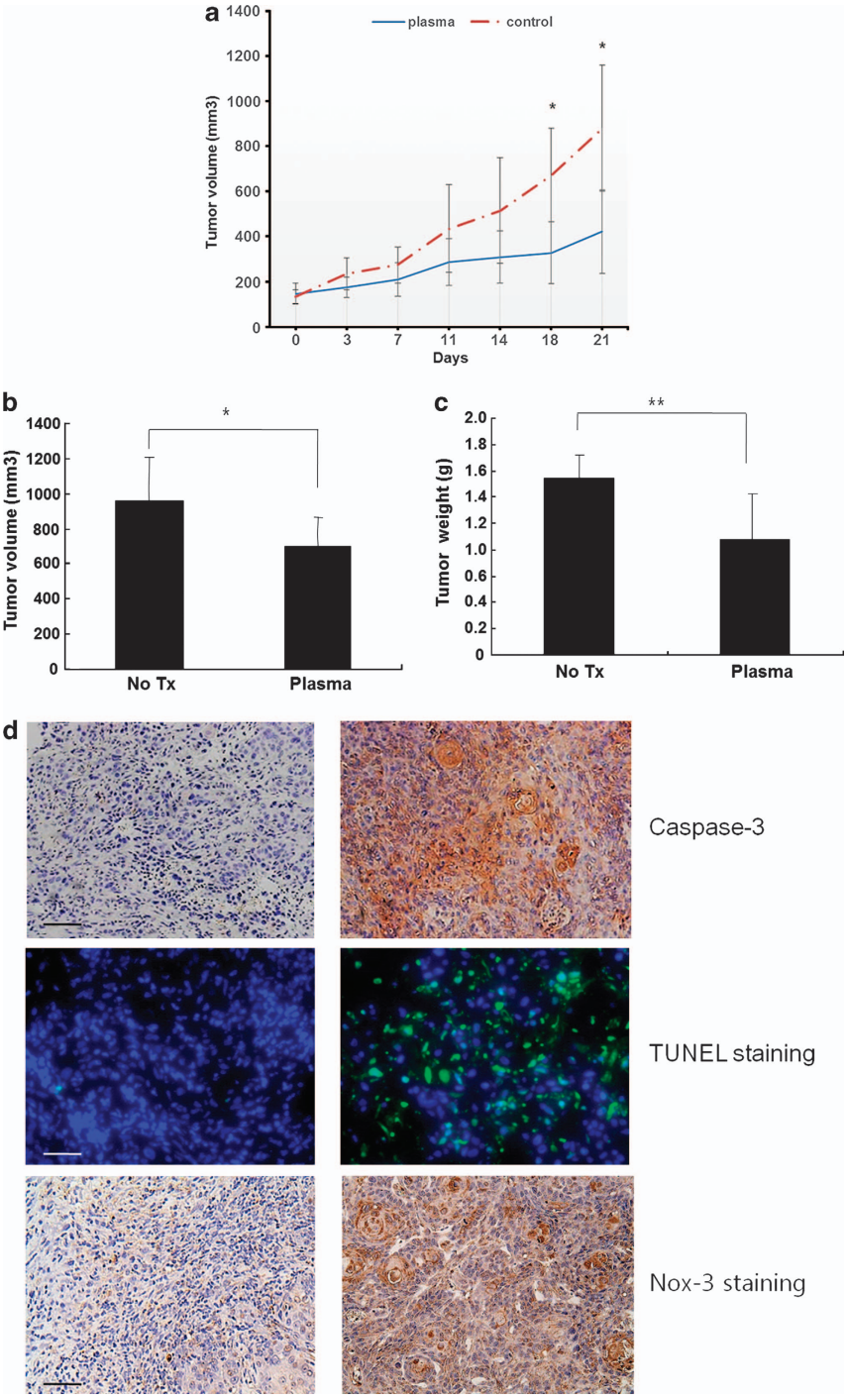

Figure 5 Effect of NTP on tumor growth and induction of apoptosis *in vivo*. (**a**) Sixteen mice were randomly divided into two groups and treated with NTP daily for 20 s. Tumor volumes were measured using a caliper two times per week. (**b**) Tumor volume and (**c**) weight were measured after they were killed. (**d**) Caspase-3, Nox-3, and TUNEL assays were performed on the tissues excised from the mice that were on day 21. Scale bar denotes 200 μm. *$P<0.05$ and **$P<0.01$

late apoptosis were quantified according to the manufacturer's instructions. Apoptosis was detected using a FACS Canto system (BD Biosciences), with the excitation and emission settings of 488 and 530 nm, respectively.

TUNEL assay. DNA fragmentation was analyzed using an *in situ* cell death detection kit (Roche Molecular Biochemicals, Basel, Switzerland), according to the manufacturer's instructions. Digital images of apoptotic cells were selected randomly under a light microscope.

Mitochondrial membrane potential assay. The MMP of intact cells was measured by flow cytometry using the lipophilic cationic probe 5,5 V,6,6 V-tetrachloro-1,1 V 3,3 V-tetra ethylbenzimidazolcarbocyanine iodide (JC-1; Molecular Probes, Eugene, OR, USA), as described previously.[19] The culture medium was briefly removed from the adherent FaDu cells, and the cells were rinsed with PBS. Cell monolayers were incubated with MEM and 5 μg/ml JC-1 at 37 °C for 20 min. The cells were subsequently washed two times with cold PBS and trypsinized. Cell pellets were then resuspended in 500 μl of PBS. The change

in MMP was measured by flow cytometry (BD Biosciences) and fluorescence microscopy (Zeiss, Jena, Germany) at 24 h after NTP.

Measurement of ROS production and localization of mitochondrial superoxide. For measurement of ROS production and mitochondrial superoxide, FaDu cells were treated with plasma for 24 h and then treated with 10 μM of 5-(and-6)-carboxy-2′,7′-dichlorodihydrofluorescein diacetate (carboxy-H_2DCFDA) dye (Molecular Probes) and MitoSOX Red (Molecular Probes), as described previously.[18] Fluorescence-stained cells (1×10^4) were then analyzed by flow cytometry. For localization of mitochondrial superoxide, cells on coverslips were exposed to 2.5 μM MitoSOX Red for 10 min and then stained with 180 nM MitoTracker Green for 20 min at 37 °C. Cells were then fixed in 4% paraformaldehyde. Image processing was performed using the fluorescence microscopy with a $\times 40$ water objective

Western blot analysis. Cells were lysed in lysis buffer containing 150 mM NaCl, 1.0% NP40, 0.5% sodium deoxycholate, 0.1% SDS, and 50 mM Tris (pH 8.0) and a protease inhibitor cocktail (Roche Molecular Biochemicals), as described previously.[20] The proteins from FaDu cells were electrotransferred to Immobilon-P membranes (Millipore Corporation, Bedford, MA, USA). Detection of specific proteins was carried out with an ECL Western blotting kit (Bio-Rad, Hercules, CA, USA) according to the manufacturer's instructions.

***In vivo* studies.** Sixteen male BALB/c nu/nu mice were purchased from Orient Bio Co. Ltd (SungNam, Korea). FaDu cells (1×10^6) resuspended in PBS were administered subcutaneously into the lower right flank of each mouse. Procedures and handling were conducted in accordance with the Committee for Ethics in Animal Experiments of the Ajou University School of Medicine. After 1 week, when tumors reached $\sim$150 mm in diameter, the mice were randomly divided into two groups (eight mice per group) and daily treatment of a single 20 s NTP, 1 cm apart from the upper margin of tumor was performed for 20 days. Tumors were measured using a sliding caliper two times per week, and the volumes (mm^3) were calculated as described previously.[18] On day 21, the tumors were excised from the mice that were killed for caspase-3, Nox-3, and TUNEL assays.

Immunohistochemistry. Caspase-3 and Nox-3 immunohistochemistry was performed on paraffin-embedded tumor sections collected on polylysine-coated slides. Briefly, the specimens were incubated with antiactive caspase-3 (Cell Signaling Technology, Beverly, MA, USA) and Nox-3 (Sigma-Aldrich, St. Louis, MO, USA) mouse primary antibody, diluted 1 : 400 in blocking solution, overnight at 4 °C. The sections were thoroughly rinsed in PBS and incubated for 2 h at room temperature with a streptavidin–biotin–peroxidase complex (Vectastain ABC Kit; Vector Laboratories, Burlingame, CA, USA). Immunolabeling was revealed after three washes in PBS using 2,3′-diaminobenzidene as a substrate, and diluted 1 : 10 in the buffer, according to the manufacturer's instructions (Roche Molecular Biochemicals). Staining was completed by incubation with 3,3-diaminobenzidine substrate chromogen, which results in a brown-colored precipitate at the antigen site. Measurements of active caspase-3- or Nox-3-positive cells were performed on 10–15 images per slide, captured by an independent observer who was blinded to the experiment.

Statistical analysis. Statistical evaluation of the data was carried out using the Student's *t*-test.

Conflict of Interest

The authors declare no conflict of interest.

Acknowledgements. This research was supported by the Bio & Medical Technology Development Program of the NRF funded by the Korean government (2012M3A9B2052870).

1. Jemal A, Siegel R, Ward E, Hao Y, Xu J, Thun MJ. Cancer statistics, 2009. *Cancer J Clin* 2009; **59**: 225–249.
2. Argiris A, Karamouzis MV, Raben D, Ferris RL. Head and neck cancer. *Lancet* 2008; **371**: 1695–1709.
3. Kim CH, Kwon S, Bahn JH, Lee K, Jun SI, Rack PD *et al.* Effects of atmospheric nonthermal plasma on invasion of colorectal cancer cells. *Appl Phys Lett* 2010; **96**: 243701.
4. Sensenig R, Kalghatgi S, Cerchar E, Fridman G, Shereshevsky A, Torabi B *et al.* Non-thermal plasma induces apoptosis in melanoma cells via production of intracellular reactive oxygen species. *Ann Biomed Eng* 2011; **39**: 674–687.
5. Kim CH, Bahn JH, Lee SH, Kim GY, Jun SI, Lee K *et al.* Induction of cell growth arrest by atmospheric non-thermal plasma in colorectal cancer cells. *J Biotechnol* 2010; **150**: 530–538.
6. Chen N, Garner AL, Chen G, Jing Y, Deng Y, Swanson RJ *et al.* Nanosecond electric pulses penetrate the nucleus and enhance speckle formation. *Biochem Biophys Res Commun* 2007; **364**: 220–225.
7. Fridman A. *Plasma Biology and Plasma Medicine Plasma Chemistry*. Cambridge University Press: Cambridge, MA, USA, 2008. pp 10.
8. Jacotot E, Ferri KF, El Hamel C, Brenner C, Druillennec S, Hoebeke J *et al.* Control of mitochondrial membrane permeabilization by adenine nucleotide translocator interacting with HIV-1 viral protein rR and Bcl-2. *J Exp Med* 2001; **193**: 509–519.
9. Droge W. Free radicals in the physiological control of cell function. *Physiol Rev* 2002; **82**: 47–95.
10. Kim K, Choi JD, Hong YC, Kim G, Noh EJ, Lee J-S *et al.* Atmospheric-pressure plasma-jet from micronozzle array and its biological effects on living cells for cancer therapy. *Appl Phys Lett* 2011; **98**: 073701.
11. Kalghatgi S, Kelly CM, Cerchar E, Torabi B, Alekseev O, Fridman A *et al.* Effects of non-thermal plasma on mammalian cells. *PLoS One* 2011; **6**: e16270.
12. Vandamme M, Robert E, Lerondel S, Sarron V, Ries D, Dozias S *et al.* ROS implication in a new antitumor strategy based on non-thermal plasma. *Int J Cancer* 2012; **130**: 2185–2194.
13. Vaux DL, Korsmeyer SJ. Cell death in development. *Cell* 1999; **96**: 245–254.
14. van Loo G, Saelens X, van Gurp M, MacFarlane M, Martin SJ, Vandenabeele P. The role of mitochondrial factors in apoptosis: a Russian roulette with more than one bullet. *Cell Death Differen* 2002; **9**: 1031–1042.
15. Green DR. Apoptotic pathways: ten minutes to dead. *Cell* 2005; **121**: 671–674.
16. Junttila MR, Li SP, Westermarck J. Phosphatase-mediated crosstalk between MAPK signaling pathways in the regulation of cell survival. *FASEB J* 2008; **22**: 954–965.
17. Kim SY, Chu KC, Lee HR, Lee KS, Carey TE. Establishment and characterization of nine new head and neck cancer cell lines. *Acta Oto-laryngol* 1997; **117**: 775–784.
18. Lee BS, Kang SU, Hwang HS, Kim YS, Sung ES, Shin YS *et al.* An agonistic antibody to human death receptor 4 induces apoptotic cell death in head and neck cancer cells through mitochondrial ROS generation. *Cancer Lett* 2012; **322**: 45–57.
19. Pyun JH, Kang SU, Hwang HS, Oh YT, Kang SH, Lim YA *et al.* Epicatechin inhibits radiation-induced auditory cell death by suppression of reactive oxygen species generation. *Neuroscience* 2011; **199**: 410–420.
20. Lim YC, Park HY, Hwang HS, Kang SU, Pyun JH, Lee MH *et al.* (−)-Epigallocatechin-3-gallate (EGCG) inhibits HGF-induced invasion and metastasis in hypopharyngeal carcinoma cells. *Cancer Lett* 2008; **271**: 140–152.